Science Arts & Métiers (SAM)

is an open access repository that collects the work of Arts et Métiers Institute of Technology researchers and makes it freely available over the web where possible.

This is an author-deposited version published in: https://sam.ensam.eu
Handle ID: .http://hdl.handle.net/10985/7493

To cite this version :

David PRAT, Guillaume FROMENTIN, Gérard POULACHON, Emmanuel DUC - Experimental Analysis and Geometrical Modeling of Cutting Conditions Effect in 5 Axis Milling with Ti6Al4V Alloy - In: 5th CIRP Conference on High Performance Cutting, Switzerland, 2012-06-04 - Procedia CIRP - 2012

Any correspondence concerning this service should be sent to the repository Administrator : scienceouverte@ensam.eu

Arts et Métiers Institute of Technology

Experimental Analysis and Geometrical Modeling of Cutting Conditions Effect in 5 Axis Milling with Ti6Al4V Alloy

David PRAT[a]*, Guillaume FROMENTIN[a], Gérard POULACHON[a], Emmanuel DUC[b]

[a]*Arts et Metiers ParisTech, LaBoMaP, Rue Porte de Paris, Cluny 71250, FRANCE*
[b]*IFMA/UBP, LaMI, Campus des Cézeaux BP265-63175 Aubière cedex, FRANCE*
* Corresponding author. Tel.: +33 385 595 344; fax: +33 385 595 370. *E-mail address*: david.prat@ensam.eu

Abstract

The 5 axis continuous milling is an advanced technique for free-form surfaces manufacturing. In finishing, this technique uses ball-end or hemispherical milling cutter. This type of operation for 5 axis milling allows the possibility to tilt the tool with two different angles. As a consequence, a mass of geometrical configurations exists and establishing accurate parameters is quite difficult to define. A geometrical model has been developed to find the effective cutting diameters and cutting speed on the cut and the finished surface. After an experimental validation, this study proposes an analysis of several 5 axis milling configurations in order to perform this technique.

© 2011 Published by Elsevier Ltd. Selection and/or peer-review under responsibility of Swiss Federal Institute of Technology

Keyword: Cutting; End milling; Effective diameter

1. Introduction

The 5 axis continuous milling is an advanced technique for free-form surfaces manufacturing. Aeronautics, spatial, and energy sectors are renowned users of complex parts such as blades, impellers or inducers, which can be made with titanium alloy [1], a difficult-to-cut material [2]. For finishing these parts, ball-end or hemispherical solid milling cutters are usually used.

This type of 5-axis milling operation is defined with different cutting conditions as the tilt & lead angles. As a consequence, a mass of geometrical configurations exists, making it quite difficult to establish adapted cutting parameters. There is a need to characterize and to model the effect of geometrical milling configurations and their consequences on the milling operation and on the obtained surface quality.

The cutting speed is one cutting conditions which characterize the cutting operation. In milling operations the spindle speed is fixed in the operation. In order to have the cutting speed on one particular point of the cutting edge, it is necessary to know the effective cutting diameter. Analytical point of view exists [3] to determine the cutting speed and the effective cutting diameter in special case with only tilt or lead angle. No generalization is possible with this approach because Boujelbene supposes that the minimum and the maximum effective cutting diameters are determined in the same plane. On the other hand, [4] had a first analytical approach but limited to the lead angle. Then, [5] and [6] had a new approach based on CAD model intersection of the part and the tool for any type of trajectory. The manufacturing program is an input data of their approach to know the cutter engagement geometry. These authors did not establish an analysis of the different milling configurations based on the effective cutting diameters.

This paper proposes to show the effect of the cutting conditions and in particular the tilt and lead angles on

the cutting speed and effective cutting diameters on the cut and the finished surfaces. The first part of the study focuses on the geometrical model of the 5 axis milling operation and the results are the effective cutting diameters for the cut and the finished surfaces. Afterwards, experimental tests are conducted in order to valid the previous model. Then, a discussion is proposed to classify the different situations of cutting conditions and milling configurations to improve the milling operation.

2. The geometrical model of the 5 axis milling operation

A hypothesis is made to establish the model. It is considered that the feed movement is negligible behind the cutting movement so the tool is modeled by its envelope.

2.1. The process coordinate system

The process coordinate system is formed by the feed T, cross-feed N, and normal surface Z. The specificity of the 5 axis milling operation is to manage the tool axis orientation in relation to the normal surface axis Z as shown in Fig 1.

In this study the axis tool orientation is defined by the tilt and lead angles as shown in Fig 1. The lead angle β_f is measured between the projection of the axis tool in the plane (N, Z) and the normal surface Z. The tilt angle β_n is positioned between the projection of the axis tool in the plane (T, Z) and the normal surface Z. The tool axis is noted Z_t.

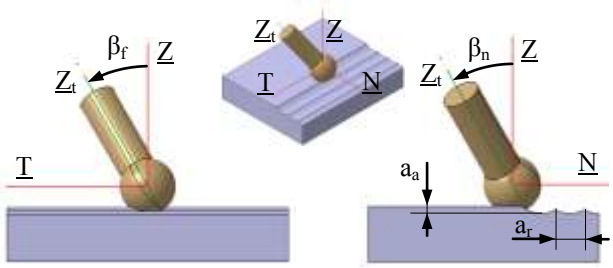

Fig. 1. Definition of the lead β_f and tilt β_n angles

The axial depth of cut a_a is determined in the Z direction between the tool's lower point and the upper surface of the part. The radial depth of cut a_r is the algebraic distance of the path between the actual tool trajectory and the previous trajectory. The radial depth of cut is positive if the surface to cut is at the right side of the plane (Z, T), when the tool goes straight ahead. Fig 1 represents a positive radial depth of cut.

The envelope of the tool is modeled by a sphere with a radius r_t equal to the tool radius and the point O as the center of the sphere. The point O has the coordinate $\{0, 0, r_t\}$ in the process coordinate system.

2.2. Definition of the cut and the finished surfaces

The scallop height R_z is calculated with the equation 1:

$$R_z = r_t - \sqrt{r_t^2 - \frac{a_r^2}{4}} \qquad (1)$$

The picturing of the colour surface is a function of the altitude of each point. All points higher than the scallop height is the surface to cut and will be cut in a next path of the tool (represented by the dark grey level) otherwise the finished surface (in lighter grey level) as in Fig 2.

The geometrical model of the part during milling (Fig 3) is composed with the actual tool path, several previous tool paths, the cut surface which is the intersection between the sphere of the tool envelope and the part and finally, the surface to cut which will be cut in a next path. Each path is modeled by a cylinder with a radius r_t. Each path is distant of the radial depth of cut a_r. The cut surface is modeled by a sphere portion represented by the white colour in the Fig 2.

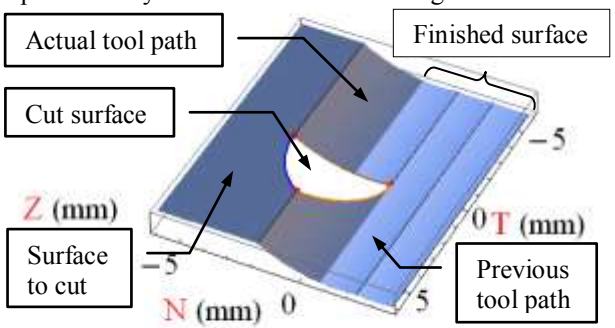

Fig. 2. The part in process with the cut and finished surfaces

3. The effective cutting diameters

3.1. Interest for the cutting speed

The cutting speed V_c (m/min) of one cutting edge point is calculated by the equation 2:

$$V_c = \frac{\pi \cdot D_{eff} \cdot N}{1000} \qquad (2)$$

In the equation 2, N is the spindle speed (rev/min) and D_{eff} is the effective cutting diameter (mm). Each point of one cutting edge of a ball-end mill has a different diameter. This effective diameter is included between the maximal diameter that is the tool diameter ($2 \times r_t$) and the minimal that is zero. The latter is obtained by the cutter location point C_L. In a 5 axis milling configuration in order to calculate the minimal and maximal cutting speed of the tool, it is necessary to know all effective cutting diameters which are in contact with the part.

3.2. The borders of the intersection between the part and the tool envelop

To obtain the effective diameters, the borders between the sphere of the cut surface and the part have to be modeled. There are 3 borders as shown in Fig 3.

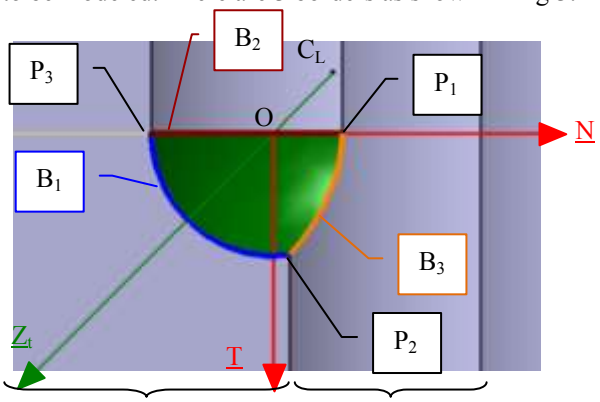

Fig. 3. The part in process with the borders of the cut surface

- Border B1: Sphere∩plane

This border is the intersection between the plane of the surface to cut located at the altitude a_a and the sphere of the tool envelope with r_t as radius. So the border B1 is a circle that can be modeled as a parameterized curve:

$$B1[\theta] = \begin{Bmatrix} \sqrt{a_a \cdot (2 \cdot r_t - a_a)} \cdot Cos(\theta) \\ \sqrt{a_a \cdot (2 \cdot r_t - a_a)} \cdot Sin(\theta) \\ a_a \end{Bmatrix} \quad (4)$$

- Border B2: Sphere∩actual tool path

This border is the intersection between the cylinder of the actual tool path with r_t as radius and the sphere of the tool envelope also with r_t as radius. So the border B2 is a circle that can be modeled as a parameterized curve:

$$B2[\theta] = \begin{Bmatrix} 0 \\ r_t \cdot Sin(\theta) \\ r_t \cdot Cos(\theta) \end{Bmatrix} \quad (3)$$

- Border B3: Sphere∩previous tool path

This border is the intersection between the cylinder of the previous path with r_t as radius and the sphere of the tool envelope also with r_t as radius. The sphere can be parameterized as the following equation:

$$Sphere[\theta, z] = \begin{Bmatrix} \sqrt{z \cdot (2 \cdot r_t - z)} \cdot Cos(\theta) \\ \sqrt{z \cdot (2 \cdot r_t - z)} \cdot Sin(\theta) \\ z \end{Bmatrix} \quad (5)$$

The cylinder of the previous tool path can be modeled in Cartesian as:

$$Prev\_Step[y, z] = \sqrt{(y - a_r)^2 + (z - r_t)^2} - r_t \quad (6)$$

So, the B3 border is obtained with the convolution of the equation 4 and 5 which allows finding a function θ[z]. As a result the border B3 is:

$$B3[z] = Sphere[\theta[z], z] \quad (7)$$

The intersection between two borders can be calculated as limit for each border. The intersection between B2∩B3, B3∩B1 and B1∩B2 generate three limit points (Fig 3) P1, P2 and P3.

3.3. The calculus of the effective cutting diameters

The distance between a point M of one border and the axis of the tool (O, $\underline{Z_t}$) is calculated by:

$$Distance[M, (O, \underline{Z_t})] = \|\underline{OM} \times \underline{Z_t}\| \quad (8)$$

The maximum effective cutting diameter is determined as twice maximum of the function *Distance* on the three borders:

$$D_{eff\ max} = 2 \cdot Maximum_i[Distance[Bi, (O, \underline{Z_t})]] \quad (9)$$

The minimum effective cutting diameter is determined as twice minimum of the function *Distance* on the three borders. But if the cutter location is in the cut surface, the minimum effective cutting diameter is equal to zero:

$$D_{eff\ min} = 2 \cdot Minimum_i[Distance[Bi, (O, \underline{Z_t})]] \quad (10)$$

All equations are implanted in Mathematica software and allow some graphical issues (Fig 4).

3.4. The effective cutting diameters generating the finished surface

In order to have more information on the milling configuration, the effective cutting diameters can be determined with changing the depth of cut equal to the scallop height (Equ. 1). That approach gives information about the effective cutting diameters machining the finished surface (Fig 4) and allowed to know the range of the cutting speed which machined the finished surface.

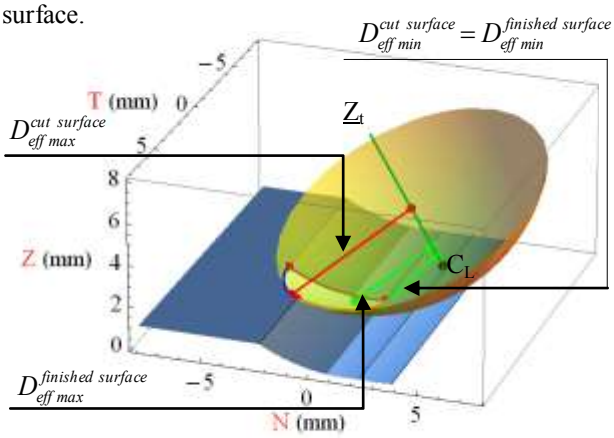

Fig. 4. Effective cutting diameters on the cut and finished surface of the configuration: r_t = 8 mm, β_t = 20°, β_n = 20°, a_r = +1.5 mm, a_a = 1 mm

3.5. Analysis of the effective cutting diameters

The observation of the different effective cutting diameters shows that in the general cases, these diameters cannot be determinate in one cross section. The existing formulas in previous study [2] can be applied to a very limited number of cases but not in the majority of cases.

4. Experimental tests

The objective of the cutting test is to validate the geometrical model. A comparison of the effective cutting diameters on the cut surface between the model and cutting tests will be achieved. The test is carried out on one linear trajectory of the tool on the part with specific cutting conditions. To measure the effective cutting diameter on the ball-end mill, yellow paint is deposited on the tool. After each cutting test two photos are taken for each tooth, a first photo of the rake face, to see precisely where the paint was removed (Fig 5) and a second photo in order to see the place where the tool was in contact with the part. The hypothesis is that the chips created on the rake face removes the yellow paint.

4.1. The condition of the tests

Experimental tests were conducted with a 5 axis milling machine ZY\XBC. The tool is a solid carbide ball-end mill Jabro 160120MEGA-64, the radius of the tool is r_t = 6 mm and has 4 teeth. The Ti6Al4V part has hardness around 33 HRc. In this situation, the recommended cutting conditions are: 3000 rev/min as spindle speed, 0.06 mm/(tooth/rev) as feed per tooth, +0.4 mm as radial depth of cut and 0.3 mm as axial depth of cut. These conditions will be the same for all the rest of the study. Under these conditions, the scallop height (Equ. 1) is R_z = 3.3 µm.

The conditions of the tests are mentioned in Table 1 with the outputs of the geometrical model. Table 1 was established by keeping constant at 45° the angle between the normal surface $\underline{Z}$ and the tool axis $\underline{Z}_t$. The last condition without tilt and lead angles is an exception. All types of tool orientations are tested. Table 1 shows the particularity of knowing the cutting speed of the cutting edge engaged in specific zones of the part. The theoretical cutting speed calculated with the tool radius r_t is 113 m/min. Of course this cutting speed is not reached. The variation of the cutting speed on the finished surface is low but in the cut surface the relative deviation is from 16% to 38% of the maximal cutting speed. The particular configuration without the tilt and lead angles demonstrates the poor level of the cutting speed in the finished surface and confirms that it is not a comfortable situation for the tool.

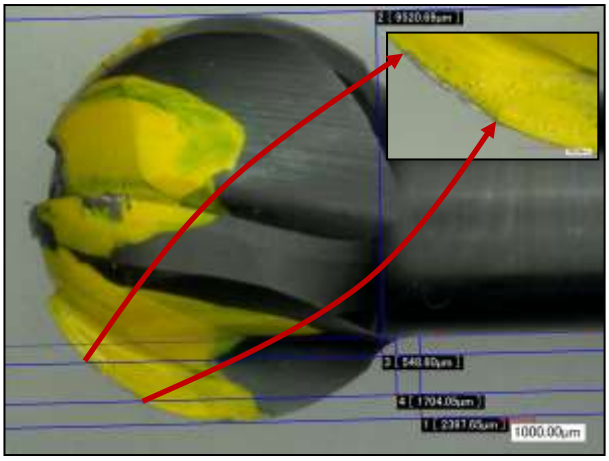

Fig. 5. Tool measurement for the condition: β_f=20°, β_n=20°

Table 1. Test conditions, outputs' model and measured effective cutting diameters linked with the cut surface

	Test	1	2	3	4	5	6	7	8	9
	β_f (°)	45	35.3	0	-35.3	-45	-35.3	0	35.3	0
	β_n (°)	0	35.3	45	35.3	0	-35.3	-45	-35.3	0
Finished surface	$D_{eff\,min}$ (mm)	8.49	8.29	8.20	8.20	8.20	8.20	8.20	8.29	0.00
	V_c (m/min)	80	78.1	77.3	77.3	77.3	77.3	77.3	78.1	0.00
	$D_{eff\,max}$ (mm)	8.76	8.77	8.76	8.69	8.49	8.69	8.76	8.77	0.40
	V_c (m/min)	82.6	82.6	82.6	81.9	80.0	81.9	82.6	82.6	3.8
Cut surface	$D_{eff\,min}$ (mm)	8.49	8.29	8.20	8.09	7.07	5.46	5.41	6.74	0.00
	V_c (m/min)	80	78.1	77.3	76.3	66.6	51.4	51.0	63.5	0.00
	$D_{eff\,max}$ (mm)	10.14	10.70	10.71	10.29	8.89	8.69	8.76	8.89	3.75
	V_c (m/min)	95.5	100.9	100.9	96.9	83.8	81.9	82.6	83.8	35.3
Measured	$D_{eff\,min}$ (mm)	8.48	9.03	8.54	8.17	6.98	5.65	5.72	6.95	0.24
	Deviation %	0.15	-8.87	-4.15	-0.96	1.22	-3.50	-5.8	-3.12	
	$D_{eff\,max}$ (mm)	10.22	10.65	10.67	10.01	8.81	8.56	8.86	9.06	3.77
	Deviation %	-0.82	0.50	0.38	2.69	0.87	1.54	-1.09	-1.84	-0.48

4.2. The result of the tests

For each test and each tooth, the measurements of the real effective cutting diameters generating the cut surface are calculated. The pictures are obtained with a digital microscope. The magnification adopted was from 20 to 50. The picture of the tool (Fig 5) shows 4 measurements relative to the tool holder and at right angles to the tool holder. A picture is not an orthogonal projection of a three dimensional object, so a linear correction has to be made in order to find the real dimension of each object.

The average of the effective cutting diameters of the four teeth are calculated and presented in Table 1. The deviation from the model in percentage is calculated between the model and the measurement divided by the model. Table 1 shows that the deviations from the model are low. The average of deviations from the model is 1.5% indicating that the geometric prediction of the effective cutting diameters on the cut surface is correct.

5. Discussion

Table 2. Situations of the uncut point for a 6 mm tool radius and 3000 rev/min of spindle speed

	Configuration	C1	C2	C3	C4
	β_f (°)	-1.5	-1.5	0	0
	β_n (°)	0	-7	-19	+19
Cut surface	$D_{eff\,min}$ (mm)	0	0	0.169	3.52
	V_c (m/min)	0	0	1.6	33.2
	$D_{eff\,max}$ (mm)	3.76	2.53	4.28	7.25
	V_c (m/min)	35.4	23.8	40.3	68.4
Finished surface	$D_{eff\,min}$ (mm)	0	1.10	3.53	3.53
	V_c (m/min)	0	10.3	33.2	33.2
	$D_{eff\,max}$ (mm)	0.51	1.88	4.28	4.28
	V_c (m/min)	4.8	17.8	40.4	40.4

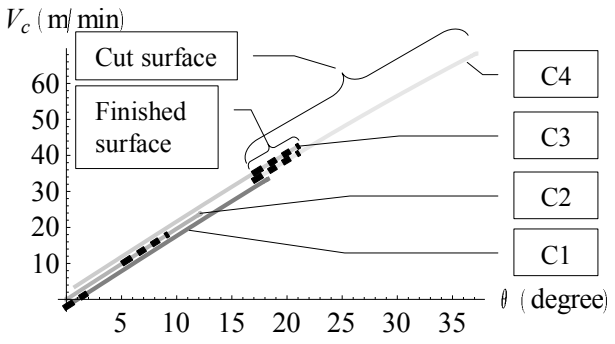

Fig. 6. Cutting speed distribution of four configurations of Table 2

The valid geometrical model of the 5 axis milling operation allows to study the different milling configurations. These configurations are classified by the situation of the cutter location C_L versus the finished surface or the cut surface. Three situations exist, the cutter location C_L engaged in: the finished surface; the cut surface (without the finished surface) and without contact with the part. Four configurations are presented in Table 2.

For each configuration 'Table 2, the cutting speed can be represented (Fig 6) as function of the θ angular position of the cutting edge profile. Each configuration is composed by the distribution of the cutting speed which corresponds to the cut surface (thick line) and the finished surface in dashed line. Each configuration curve is drawn with a little offset in Fig 6 in order to discriminate the different cases.

5.1. The cutter location engaged in the finished surface

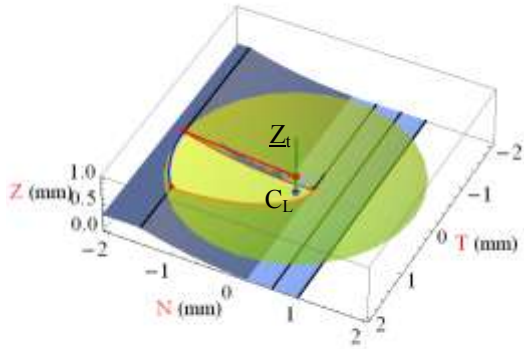

Fig. 7. Configuration C1: β_f = -1.5°, β_n = 0°

This situation exists when the minimum effective cutting diameter on the finished surface is nil (Fig 7). The geometrical consequence is that the tilt and lead angles are small. This configuration is used with the 3 axis milling machine when the tool has a trajectory perpendicular to the spindle axis. In that case the tilt and lead angles are nil.

In the entire finished surface (Tab. 2), the maximum cutting speed (4.8 m/min) is only 4% of the cutting speed (113 m/min) at the tool radius (6 mm). [6] shows that this configuration induces compression residual stresses in steel finished surface and the low kinematic condition is not disconnected with the mechanical load.

5.2. The cutter location engaged in the cut surface

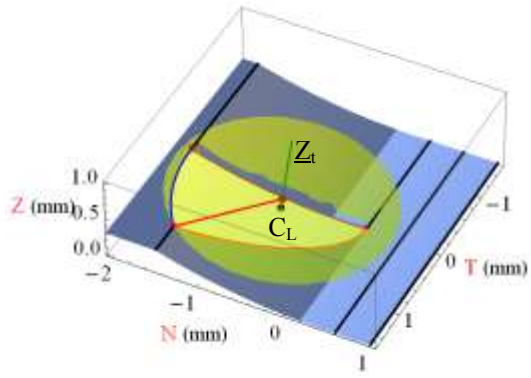

Fig. 8. Configuration C2: β_f = -1.5°, β_n = -7°

This situation exists when the minimum effective cutting diameter is nil on the cut surface but not on the finished surface (Fig 8). In the finished surface, the cutting speed is acceptable (Tab. 2). However all the effective cutting diameters lower than the minimum effective cutting diameter of the finished surface generate a very low cutting speed as the situation illustrated in Fig 6.

5.3. The cutter location without contact with the part

This last situation covers a large choice of cutting conditions. However two groups of different configurations can be made depending on the cutting speed in the finished surface.

- The uncut point is without contact and has a higher cutting speed on the finished surface

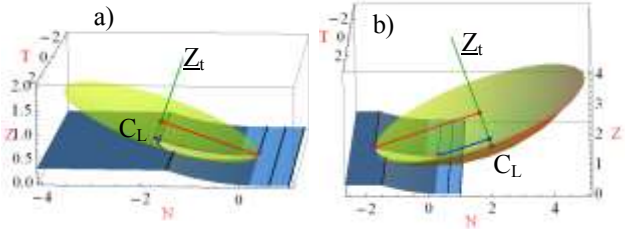

Fig. 9. Configurations: (a) C3 (β_f= 0°, β_n= -19°); (b) C4 (β_f= 0°, β_n= +19°)

This situation (Fig 9a) results in a higher cutting speed in the finished surface, so the final machined surface is obtained with a better roughness quality surface than the surface of the actual path who is at higher altitude than the scallop height. The average roughness is about 0.22 µm in the finished surface versus 1.06 µm in the cut surface. The global range of cutting speed is lower than the situation with the configuration C4 in the Fig 6.

- The uncut point is without contact and has a lower cutting speed on the finished surface

This final situation (Fig 9b) results in the cutter location under the surface to cut. This geometrical configuration produces a lower cutting speed in the finished surface.

In this case the criteria of the division of the maximum by the minimum cutting speed in the cut surface (Tab. 2) is lower than the previous situation with the higher cutting speed in the finished surface. Furthermore the range of the cutting speed in the finished surface is the same as the configuration C3. In conclusion this final situation presents a better global cutting speed because of the geometrical configuration.

6. Conclusion

The geometrical model of the 5 axis milling operation demonstrates the influence of the tilt and lead angles on the effective cutting diameter and the cutting speed. This model allows to distinct the situation of the cutting speed in the cut surface versus the finished surface. Some experimental measurements of the effective cutting diameters on the cut surface prove that the 5 axis geometrical model is a good methodology to specify the configuration. Several 5 axis milling configurations have been analysed based on the position of the cutter versus the part. When the cutter is in contact with the part, on the finished surface or the cut surface, the range of the cutting speeds are low. When the cutter is without contact of the part, several configurations exist. If the objective is to have the higher cutting speed, then the configurations with the cutter under the finished surface is the best choice.

The Ti6Al4V alloy is a difficult to cut material so precise cutting conditions have to be chosen as [2]. This model is created to determine the conditions adapted to the 5 axis milling operation. The surface quality of the part is the consequence of the local cutting condition effect in the finished surface but also on the milling mode and the cutting forces. They will be investigated.

References

[1] Boyer RR, 1996, An overview on the use of titanium in the aerospace industry, Materials Science and Engineering, Vol.213, No1-2, August 1996, pp.103-114.

[2] Corduan N, Himbert T, Poulachon G, Dessoly M, Lambertin M, Vigneau J, et al., 2003,Wear mechanisms of new tools materials for Ti-6Al-4V high performance machining, CIRP Annals – Manufacturing Technology, Vol.52, No.1, pp.73-76.

[3] Boujelbene M, Moisan A, Bouzid W, Torbaty S, 2007, Variation cutting speed on the five axis milling, Journal of Achievements in Materials and Manufacturing Engineering, JAMME, Vol.21/2 April 2007, pp.7-14.

[4] Ozturk E, Lazoglu I, 2006, Machining of free-form surfaces. Part I: Analytical chip load, International Journal of Machine Tools and Manufacture, Vol.46, pp.728-735.

[5] Lazoglu I, Boz Y, Erdim H, 2011, Five-axis milling mechanics for complex free form surfaces, CIRP Annals – Manufacturing Technology, Vol.60, pp.117-120.

[6] Ozturk E, Taner Tunc L, Budak E, 2009, Investigation of lead and tilt angle effects in 5-axis ball-end milling processes, International Journal of Machine Tools and Manufacture, Vol.49, pp.1053-1062.

[7] Guillemot N, Beaubier B, Braham T, Lartigue C, Billardon R, 2011, A hybrid approach to predict residual stresses induced by ball-end tool finishing milling of a bainitic steel, Advanced Materials Research, Vol.223, pp.391-400.